Inventory of Supplemental Information

Figure S1. Related to Figure 1. Figure S1 shows data demonstrating a requirement for piRNAs and piRNA-dependent siRNAs in fertility.

Figure S2. Related to Figure 3. Figure S2 shows small RNA sequencing data from animals in which endogenous RNAi was reset in the presence or absence of piRNAs.

Figure S3. Related to Figure 4. Figure S3 shows a variety of small RNA sequencing data, qPCR data, and protein localization data demonstrating that mRNAs are missorted between the CSR-1 and WAGO pathways after resetting endogenous RNAi in the absence of piRNAs.

Table S1. Related to Figure 3. Table S1 contains small RNA sequencing data for transposons after endogenous RNAi was reset in the presence or absence of piRNAs.

Table S2 (Tabs 1-4). Related to Figure 4. Table S2 contains small RNA sequencing data for genes that yield siRNAs enriched in FLAG::HRDE-1 IP or GFP::CSR-1 IP after resetting endogenous RNAi in the presence or absence of piRNAs.

Supplemental Experimental Procedures.

Supplemental References.

SUPPLEMENTAL FIGURES

A

Fertility of F2 progeny after resetting RNAi in the absence of piRNAs (*prg-1-/-*)

mut-16 genotype	*mut-14 smut-1* genotype	Fertile	Sterile
mut-16-/-	*mut-14-/- smut-1-/-*	1	0
mut-16-/-	*mut-14+/+ smut-1+/+* or *mut-14+/- smut-1+/-*	7	0
mut-16+/+ or *mut-16+/-*	*mut-14-/- smut-1-/-*	14	0
mut-16+/+ or *mut-16+/-*	*mut-14+/+ smut-1+/+* or *mut-14+/- smut-1+/-*	1	20
mut-16+/+	*mut-14+/- smut-1-/-* (recombinant)	0	1
mut-16+/-	*mut-14-/- smut-1+/-* (recombinant)	1	0

B

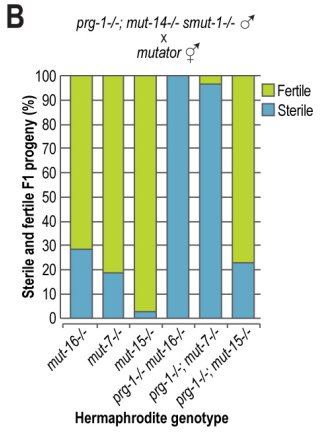

C

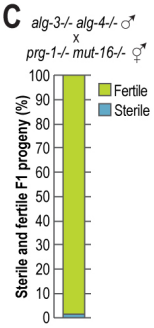

D

Gene inactivations tested for rescue of sterility caused by resetting endogenous RNAi in the absence of piRNAs

RNAi treatment	Gene description	Fertile animals
control	Empty vector	1%
hrde-1	Argonaute/nuclear RNAi	52%
daf-2	Insulin receptor	0%
ced-3	Caspase/apoptosis	0%
ced-4	Novel/apoptosis	0%
cep-1	p53/DNA damage-induced apoptosis	0%
hus-1	Hus1/DNA damage-induced apoptosis	0%
rad-54	Rad54/DNA damage-induced apoptosis	0%
pch-2	PCH2/asynapsis-induced apoptosis	0%
atl-1	ATM/DNA-damage checkpoint	0%
chk-1	Chk1/DNA-damage checkpoint	0%
mrt-2	RAD1/DNA-damage checkpoint	0%
brc-2	BRCA2/DNA repair	0%
eri-1	Exonuclease/26G-RNA formation	0%

Figure S1. Related to Figure 1. Fertility defects after resetting endogenous RNAi. **(A)** Genotype and fertility of the F2 progeny of fertile F1 animals after resetting RNAi in the absence of piRNAs (*prg-1-/-; mut-14-/- smut-/-* males crossed to *prg-1-/- mut-16-/-* hermaphrodites). **(B)** The proportions of fertile and sterile F1 progeny from crosses between *mut-14-/- smut-1-/-* males and hermaphrodites containing mutations in the indicated *mutator* genes in the presence or absence of piRNAs (*prg-1+/+* or *prg-1-/-*). **(C)** The proportions of fertile and sterile F1 progeny from a cross between *alg-3-/- alg-4-/-* males and *prg-1-/- mut-16-/-* hermaphrodites. **(D)** The percentage of fertile F1 animals after resetting RNAi in the absence of piRNAs (*prg-1-/-; mut-14-/- smut-/-* males crossed to *prg-1-/- mut-16-/-* hermaphrodites) while inactivating each gene indicated by RNAi treatment during the P0 and F1 generations.

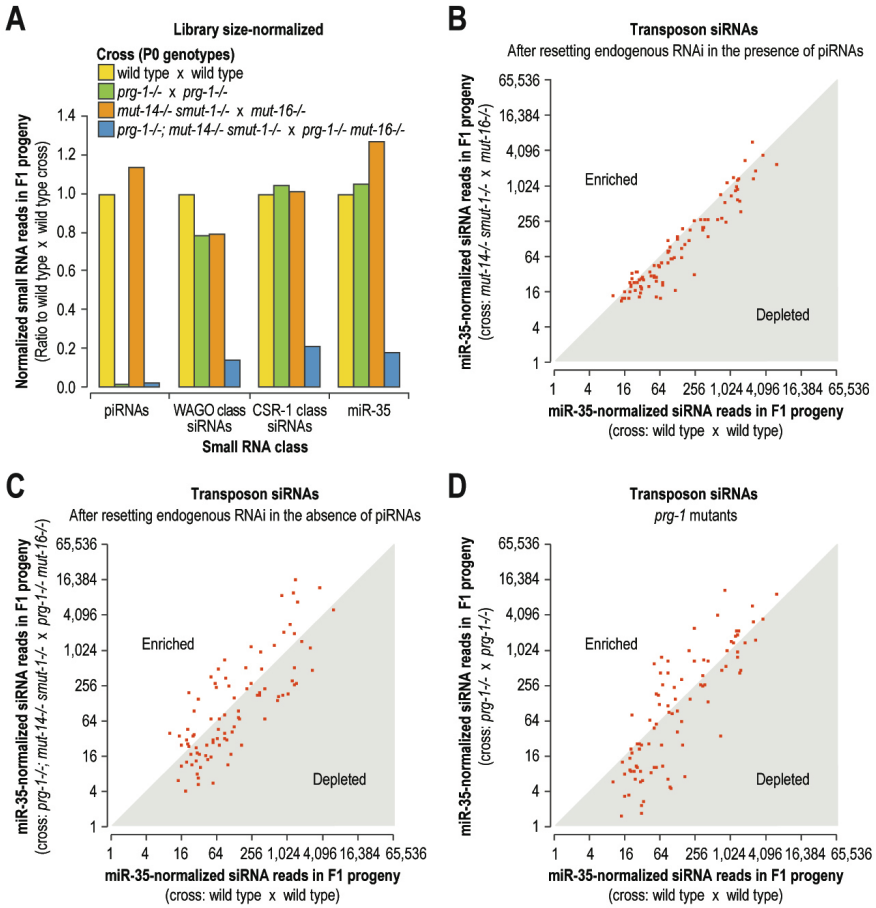

Figure S2. Related to Figure 3. Small RNA profiling after resetting endogenous RNAi. **(A)** Levels of piRNAs, WAGO class siRNAs, CSR-1 class siRNAs, and miR-35 after resetting RNAi in the presence or absence of piRNAs. F1 progeny from wild type and *prg-1* crosses are also shown. Small RNA reads were normalized to the total number of genome-matching reads in each library (unlike in Figure 3 in which reads were normalized to total miR-35 reads). **(B-D)** Unlike in A, reads were normalized to miR-35 levels (reads per 10,000 miR-35 reads). **(B)** Each transposon is shown as the number of siRNA reads after resetting RNAi in the presence of piRNAs (y-axis) relative to the levels of siRNA reads in the F1 progeny of a wild type control cross (x-axis). **(C)** Each transposon is shown as the number of siRNA reads after resetting RNAi in the absence of piRNAs (y-axis) relative to the levels of siRNA reads in the F1 progeny of a wild type control cross (x-axis). **(D)** Each transposon is shown as the number of siRNA reads in the F1 progeny of a *prg-1* x *prg-1* cross (y-axis) relative to a wild type control cross (x-axis).

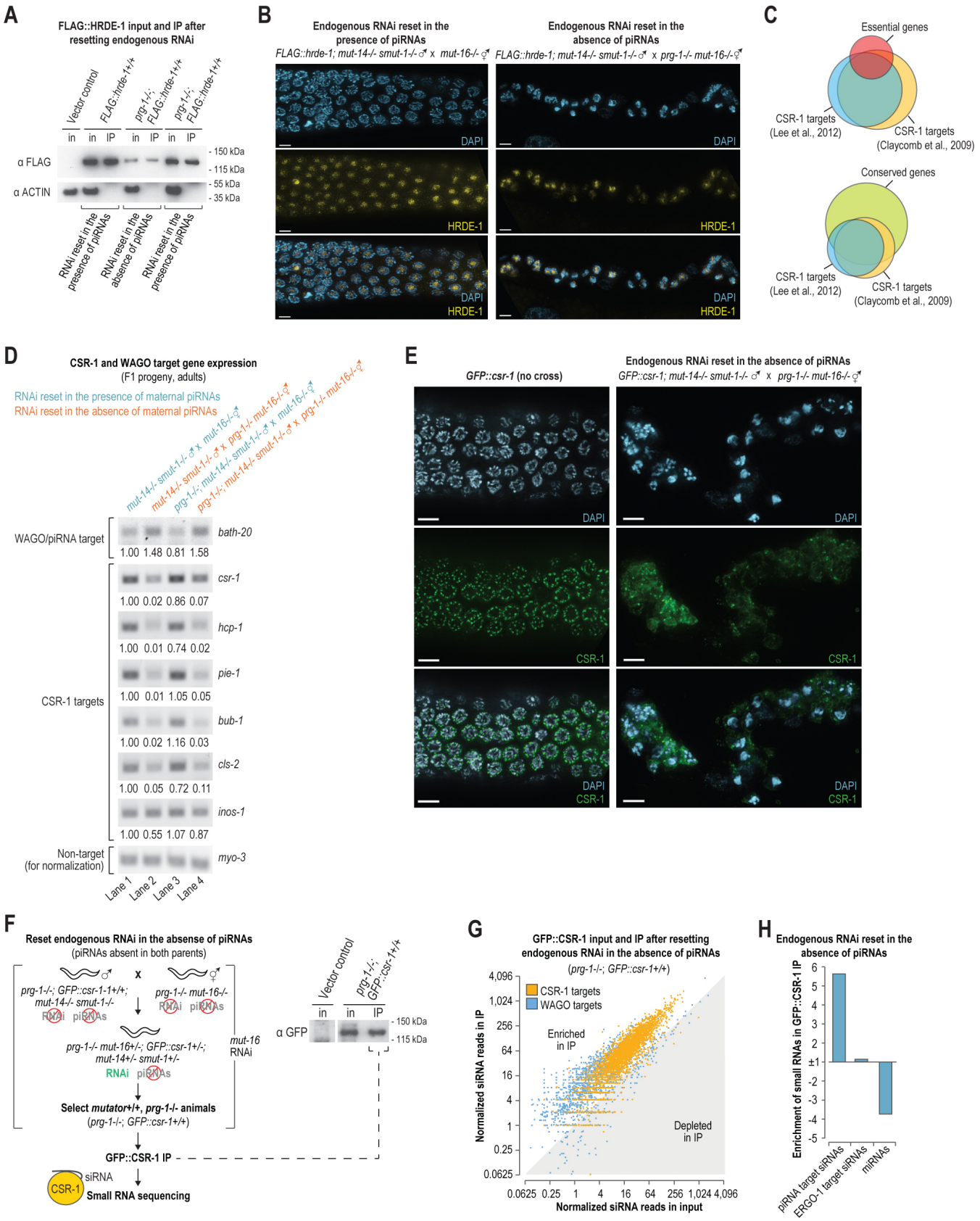

Figure S3. Related to Figure 4. Missorting of mRNAs between the CSR-1 and WAGO pathways after resetting endogenous RNAi in the absence of piRNAs. **(A)** Western blot analysis of FLAG::HRDE-1

after resetting RNAi in the presence or absence of piRNAs. Cell lysates (input) and FLAG::HRDE-1 immunoprecipitates (IP) are shown (all but the vector control is also shown in Figure 4B). See figure 4 and the main text for a description of the lines. **(B)** FLAG::HRDE-1 localization after resetting RNAi in the presence or absence of piRNAs. DNA was stained with DAPI. All images are projections of 3D images following deconvolution. Scale bars represent 5 μm. **(C)** The Venn diagrams display the overlap between essential and conserved genes and CSR-1 targets. **(D)** qPCR analysis of CSR-1 target mRNAs and the piRNA target mRNA *bath-20* after resetting RNAi in the presence (lanes 1 and 3) or absence (lanes 2 and 4) of maternal piRNAs. Gel images display PCR products for each gene in the F1 progeny of the crosses indicated. The relative levels were calculated using SYBR Green qRT-PCR, except for *bath-20*, which was below the threshold for detection in our SYBR Green assay and was instead calculated by quantifying the signal on an Agarose gel. **(E)** GFP::CSR-1 localization in control (non-mutant) animals and after resetting RNAi in the absence of piRNAs. DNA was stained with DAPI. All images are projections of 3D images following deconvolution. Scale bars represent 5 μm. **(F)** Schematic illustrating the approach used to reset endogenous RNAi and then immunoprecipitate (IP) GFP::CSR-1 and sequence the associated small RNAs. Animals of the indicated genotype were selected for GFP::CSR-1 IP and small RNA sequencing after resetting RNAi in the absence of piRNAs. Animals were treated with *mut-16* RNAi to prevent efficient reactivation of RNAi while they were genotyped and expanded. The western blot displays GFP::CSR-1 protein in the input (in) and IP. **(G)** Each CSR-1 and WAGO target is represented as the number of normalized siRNA reads in the GFP::CSR-1 input (x-axis) and IP (y-axis) fractions after resetting RNAi in the absence of piRNAs. **(H)** Enrichment or depletion of siRNAs from piRNA targets or ERGO-1 targets and miRNAs in the GFP::CSR-1 IP relative to the input.

SUPPLEMENTAL TABLE LEGENDS (Tables are available as separate Excel documents)

Table S1. Related to Figure 3. siRNA reads derived from transposons (Repbase) in the F1 progeny of the indicated crosses.

Table S2. Related to Figure 4. Small RNA sequencing data for genes that yield siRNAs enriched in FLAG::HRDE-1 or GFP::CSR-1 IPs. **(Tab 1)** Genes yielding siRNAs enriched in FLAG::HRDE-1 IP after resetting endogenous RNAi in the presence of piRNAs (*prg-1+/+*). Genotype, *FLAG::hrde-1+/+.* **(Tab 2)** Genes yielding siRNAs enriched in FLAG::HRDE-1 IP after resetting endogenous RNAi in the presence of piRNAs (*prg-1+/-*). Genotype, *prg-1-/-; FLAG::hrde-1+/+*. **(Tab 3)** Genes yielding siRNAs enriched in FLAG::HRDE-1 IP after resetting endogenous RNAi in the absence of piRNAs (*prg-1-/-*). Genotype, *prg-1-/-; FLAG::hrde-1+/+*. **(Tab 4)** Normalized siRNA reads mapping to piRNA targets in GFP::CSR-1 input and IP after resetting endogenous RNAi in the absence of piRNAs. Genotype, *prg-1-/-; GFP::csr-1+/+.*

SUPPLEMENTAL EXPERIMENTAL PROCEDURES

Strains

The following strains were used in this study: N2 [wild-type], HT1593 [*unc-119(ed3) III*], SX922 [*prg-1(n4357) I*], GR2114 [*prg-1(n4357) I; unc-119(ed3) III*], NL1810 [*mut-16(pk710) I*], GR2068 [*mut-16(pk710); unc-119(ed3) III*], GR2115 [*prg-1(n4357) mut-16(pk710) I*], GR2069 [*prg-1(n4357) mut-16(pk710) I; unc-119(ed3) III*], GR1948 [*mut-14(mg464) smut-1(tm1301) V*], GR2070 [*prg-1(n4357) I; mut-14(mg464) smut-1(tm1301) V*], GR2108 [*mut-7(pk720) unc-119(ed3) III*], GR2109 [*prg-1(n4357) I; mut-7(pk720) unc-119(ed3) III*], GR2110 [*unc-119(ed3) III; mut-15(tm1358) V*], GR2111 [*prg-1(n4357) I; unc-119(ed3) III; mut-15(tm1358) V*], GR2112 [*flag::hrde-1 II; unc-119(ed3) III; mut-14(mg464) smut-1(tm1301) V*], GR2113 [*prg-1(n4357) I; flag::hrde-1 II; unc-119(ed3) III; mut-14(mg464) smut-1(tm1301) V*], GR2119 [*prg-1(n4357) I; neSi9[GFP::csr-1] II; unc-119(ed3) III; mut-14(mg464) smut-1(tm1301) V*], WM239 [*neSi9[GFP::csr-1] II; unc-119(ed3) III*], and WM200 [*alg-3(tm1155); alg-4(ok1041)*].

RNA isolation and quantitative RT-PCR

For analysis of total small RNAs and select mRNAs after resetting RNAi in the presence or absence of piRNAs, genetic crosses were done as indicated in Figures 3 and S3D and 2-4 day adult F1

progeny were collected by hand picking crossed animals. Total RNA was isolated using Trizol (Life Technologies) followed by chloroform extraction and isopropanol precipitation. Reverse transcription was done using SuperScript III (Life Technologies). Quantitative RT-PCR was done using iTaq Universal SYBR Green Supermix (Bio-Rad) according to the manufacturer's recommendations and the following primers: myo-3 (GACTGACGGAATTGGTTGAC and GCTCTCTCTTCAGCTTGTTC), csr-1 (CGTATGCAGTCTTCATCAGC and GCTATAGGAGAGTTGAGTGG), hcp-1 (GATGCTAAACCTCGTGCAAG and CTTTCTGAGAGAGTGCTTCC), bub-1 (GTTGTGAAGGAAGTCCATGC and CTGTCGTTACTCATCAGAGC) inos-1 (GTTGCTGATTCGAAGAGAGC and GTCGACTTTGTAGGAGACAC), cls-2 (GATGGCAGATCAGAGGAATG and GTTGATCATGTCCGTGAGAC), pie-1 (GATCGAGTTCTTCAGCATCG and GTGAATGAAGCGGCATCTTG), and bath-20 (GCTCTCAAGCATGAGATTCTGC and CTTCGCGATTTTGACTCGATCC). Three technical replicates were done for each qPCR assay. Because of the time and effort required to hand pick animals, biological replicates were not done, however, the four strains used in the study correspond to two independent strains in which RNAi was reset in the presence of piRNAs and two independent strains in which RNAi was reset in the absence of piRNAs. Relative mRNAs levels were quantified using the $2^{-\Delta\Delta ct}$ method, except for *bath-20*, which was below the threshold for detection in our SYBR Green assay and was instead quantified by band intensity on an Agarose gel.

Protein-RNA immunoprecipitation and western blot assays

GFP::CSR-1 and FLAG::HRDE-1 were immunoprecipitated from adult animals 68 hours post L1 synchronization. Cells were lysed in 50 mM Tris-Cl, pH 7.5, 100 mM KCl, 2.5 mM $MgCl_2$, 0.1% Igepal CA-630, 0.5 mM PMSF, and 1X Roche Complete Proteinase Inhibitor. Cell debris was removed by centrifugation and lysates were incubated with antibodies against GFP (Life Technologies, A11120) or FLAG (Sigma, F1804) for 30 min followed by Protein A Agarose beads (Roche, 11134515001) for 30 min to capture Argonaute-small RNA complexes. Beads containing the protein-RNA complexes were washed 5 times for 10 min each to remove contaminating RNA and proteins. All steps were done at

4˚C. Protein samples for western blot analysis were taken from the cell lysate (input) and Protein A Agarose beads following immunoprecipitation (IP). Small RNAs were isolated from the remaining input and IP samples using Trizol (Life Technologies) followed by chloroform extraction and isopropanol precipitation. Western blots were done with 4-12% Bis-Tris polyacrylamide precast gels (Life Technologies). GFP::CSR-1 protein was detected using GFP antibody (Pierce, MA5-15256-HRP) and FLAG::HRDE-1 protein was detected using FLAG antibody (Sigma, F1804).

High-throughput sequencing

18-30-nt long RNAs were size selected on 17% polyacrylamide gels, treated with Tobacco Acid Phosphatase or RNA 5' Polyphosphatase (Epicentre) to reduce 5’ di- and triphosphate groups to monophosphates, ligated to 3’ and 5’ adapters, reverse transcribed, and PCR amplified. A detailed protocol is available on request. The TruSeq small RNA PCR Indexing primers RPI1-12 were used to introduce index sequences prior to multiplexed sequencing using an Illumina HiSeq 2000 machine. Small RNA sequences were parsed from adapters and mapped to the *C. elegans* genome (Wormbase release WS230) using CASHX v. 2.3 (Fahlgren et al., 2009). Data analysis was done with custom Perl scripts, R, and Excel. WAGO targets were defined as genes that yield ≥10 reads per million total genome-matching reads and that were depleted by ≥3 fold in *mut-16* mutant animals, relative to wild type. The majority (96%) of WAGO targets were also depleted of siRNAs ≥3 fold in *mut-14 smut-1* mutants. CSR-1 targets were defined as genes that produce siRNA that bind CSR-1 (Claycomb et al., 2009; Lee et al., 2012; Phillips et al., 2012). For FLAG::HRDE-1 and GFP::CSR-1 input and IP small RNA sequencing data analysis, small RNA reads were normalized to the total genome-matching reads and enrichment was determined by comparing the normalized reads in the IP to the normalized reads in the input.

Immunostaining and imaging

C. elegans were dissected in egg buffer containing 0.1% Tween-20 and fixed in methanol as described (Phillips et al., 2009). Samples were immunostained with guinea pig anti-HTP-3

(MacQueen et al., 2005), mouse anti-PGL-1 (K76) (Strome and Wood, 1983), rabbit anti-GFP (Invitrogen, A11122) or mouse anti-FLAG (Sigma, F1804). Alexa-Fluor secondary antibodies were purchased from Life Technologies. All animals were dissected within the first 24 h after L4. Images were acquired on an Axio Imager Z1 (Zeiss Microscopy) microscope or a Deltavision Elite (GE Life Sciences). 3D image stacks were collected and processed by iterative deconvolution using Axiovision (Zeiss Microscopy) or Softworx (GE Life Sciences) software. Three-dimensional images are presented as maximum intensity projections.

SUPPLEMENTAL REFERENCES

Claycomb, J.M., Batista, P.J., Pang, K.M., Gu, W., Vasale, J.J., van Wolfswinkel, J.C., Chaves, D.A., Shirayama, M., Mitani, S., Ketting, R.F., et al. (2009). The Argonaute CSR-1 and its 22G-RNA cofactors are required for holocentric chromosome segregation. Cell *139*, 123–134.

Fahlgren, N., Sullivan, C.M., Kasschau, K.D., Chapman, E.J., Cumbie, J.S., Montgomery, T.A., Gilbert, S.D., Dasenko, M., Backman, T.W.H., Givan, S.A., et al. (2009). Computational and analytical framework for small RNA profiling by high-throughput sequencing. Rna *15*, 992–1002.

Lee, H.-C., Gu, W., Shirayama, M., Youngman, E., Conte, D., and Mello, C.C. (2012). C. elegans piRNAs Mediate the Genome-wide Surveillance of Germline Transcripts. Cell *150*, 78–87.

MacQueen, A.J., Phillips, C.M., Bhalla, N., Weiser, P., Villeneuve, A.M., and Dernburg, A.F. (2005). Chromosome sites play dual roles to establish homologous synapsis during meiosis in C. elegans. Cell *123*, 1037–1050.

Phillips, C.M., McDonald, K.L., and Dernburg, A.F. (2009). Cytological analysis of meiosis in Caenorhabditis elegans. Methods Mol. Biol. *558*, 171–195.

Phillips, C.M., Montgomery, T.A., Breen, P.C., and Ruvkun, G. (2012). MUT-16 promotes formation of perinuclear Mutator foci required for RNA silencing in the C. elegans germline. Genes Dev *26*, 1433–

1444.

Strome, S., and Wood, W.B. (1983). Generation of asymmetry and segregation of germ-line granules in early C. elegans embryos. Cell *35*, 15–25.